8-2024

Task scheduling strategy for 3DPCP considering multidynamic information perturbation in green scene

JianJia HE

Jian WU

Keng SIAU
Singapore Management University, klsiau@smu.edu.sg

Journal of Global Information Management
Volume 32 • Issue 1 • January-December 2024

Task Scheduling Strategy for 3DPCP Considering Multidynamic Information Perturbation in Green Scene

JianJia He
Business School, University of Shanghai for Science and Technology, China & Supper Network Research (China) Centre, University of Shanghai for Science and Technology, China

Jian Wu
Business School, University of Shanghai for Science and Technology, China

Keng Leng Siau
Department of Information Systems, City University of Hong Kong, China

ABSTRACT

The 3D printing cloud platform (3DPCP) plays a pivotal role in breaking down the information silos between supply and demand, effectively reducing waste through information integration and intelligent production. However, due to the complexity of 3DPCP scheduling in green scenes and the multidynamic information perturbations, unveils problems in traditional task scheduling methods in 3DPCP. These issues manifest as incomplete considerations, subpar green performance, and weak adaptability to dynamic changes. There is an urgent need to design practical methods to realize the multidynamic information perturbations in green scenes within 3DPCP. Therefore, this article first defines the 3DPCP task scheduling problem for multidynamic information perturbation in green scenes. Second, the article proposes a task scheduling model and a heuristic task scheduling strategy to minimize both the average cost and carbon dioxide (CO2) emissions per unit of quality product. Finally, the article validates effectiveness and superiority of the proposed strategy through simulation experiments.

KEYWORDS

Green Scene, Multidynamic Information, 3D Printing Cloud Platform (3DPCP), Task Scheduling, Heuristic Scheduling Strategy

TASK SCHEDULING STRATEGY FOR 3D PRINTING CLOUD PLATFORM CONSIDERING MULTI-DYNAMIC INFORMATION PERTURBATION IN GREEN SCENE

The three-dimensional printing cloud platform (3DPCP) is an online service platform based on 3D printing technology, facilitating efficient collaboration with multiple entities, including demand, production, and logistics (Cui et al., 2022). Among them, 3D printing (3DP) is a disruptive technology boasting not only production advantages such as high digitization, rapid prototyping, and print-on-demand but also environmental advantages like low energy consumption and minimal material waste (Karimi & Ning, 2021; Sgarbossa et al., 2021; Srinivasan et al., 2018). Moreover, cloud platforms serve as service platforms combining technologies like cloud computing and the

DOI: 10.4018/JGIM.351156

Internet, characterized by resource optimization and fostering green and sustainable manufacturing processes (Feng et al., 2022; Lin & Ma, 2022; Wu et al., 2022). With the rapid development of emerging technologies, the application of 3DPCP continues to grow (Zhong et al., 2022). Industry players like Xometry have established an extensive network of manufacturer partnerships, providing convenient 3DP manufacturing services to various customers (Wu et al., 2022). Similarly, platforms like 3D Hubs, Shapeways, Sculpteo, and Quickparts provide cloud-based 3DP services (Darwish et al., 2021).

As the global market evolves and competition escalates, how manufacturing companies improve their competitiveness has become a critical issue (Zhang et al., 2024). Scheduling serves as a key means to achieve the goals of cloud platforms and promote sustainable manufacturing (Alvarez-Meaza et al., 2021; Liu et al., 2019). Many scholars have researched 3DPCP scheduling. Still, various challenges persist in addressing multi-dynamic information perturbations in green scenes. Compared with traditional approaches, scheduling tasks in 3DPCP within green scenes has several characteristics:

1. **Resource and task distribution:** Task scheduling in green scenes aims to coordinate customer-uploaded tasks with resources provided by suppliers, necessitating a resource and task-distributed 3DPCP model.
2. **Integration of 3DP and environmental material production:** Deeper integration of the 3DP manufacturing industry with eco-friendly materials will lead to a diversity of materials. Therefore, attributes like material and accuracy must be considered in the scheduling process.
3. **Interconnection with the clean energy industry:** The interconnection of the clean energy industry with the 3D printing manufacturing industry can respond to energy efficiency needs. However, clean energy availability varies geographically, requiring task scheduling adjustments based on the availability of clean energy (Tan & Lin, 2023).
4. **Integration with the logistics industry:** Green scenes will drive the integration of the logistics industry with 3DPCP, necessitating closer coordination between production and transportation. This will require more efficient task-scheduling strategies.
5. **Autonomous handling of dynamic information:** Traditional scheduling methods usually address task scheduling under the real-time arrival of order information. However, considering multi-dynamic information perturbations, 3DPCP should autonomously deal with dynamic information, such as order arrivals and cancellations, device additions and failures, and device time-window changes for intelligent manufacturing.

To clarify the relationship between multiple entities in green scenes, we constructed the 3DPCP task scheduling framework considering multi-dynamic information perturbations (see Figure 1). This framework involves customers uploading orders at random times, suppliers virtualizing resources on the cloud platform's resource layer, and real-time adjustments through the platform and its services. Highlighting the 3DPCP task scheduling characteristics in green scenes and the multi-dynamic information perturbation in 3DPCP leads to incomplete considerations, poor green performance, and poor dynamics in the traditional 3DPCP task scheduling methods. Therefore, there is an urgent need to explore 3DPCP task scheduling methods considering multi-dynamic information perturbations in green scenes.

The article is organized as follows: The next section provides an overview of related work in the field. Section 3 defines the problem of 3DPCP task scheduling considering multi-dynamic information perturbations in green scenes. Sections 4 and 5 present the development of a task scheduling model and a heuristic task scheduling strategy, respectively. Section 6 outlines the design of simulation experiments and analyzes the experimental results. Finally, Section 7 encapsulates the findings, draws conclusions, and outlines future research directions.

Figure 1. 3DPCP task scheduling framework considering multi-dynamic information perturbation in green scene

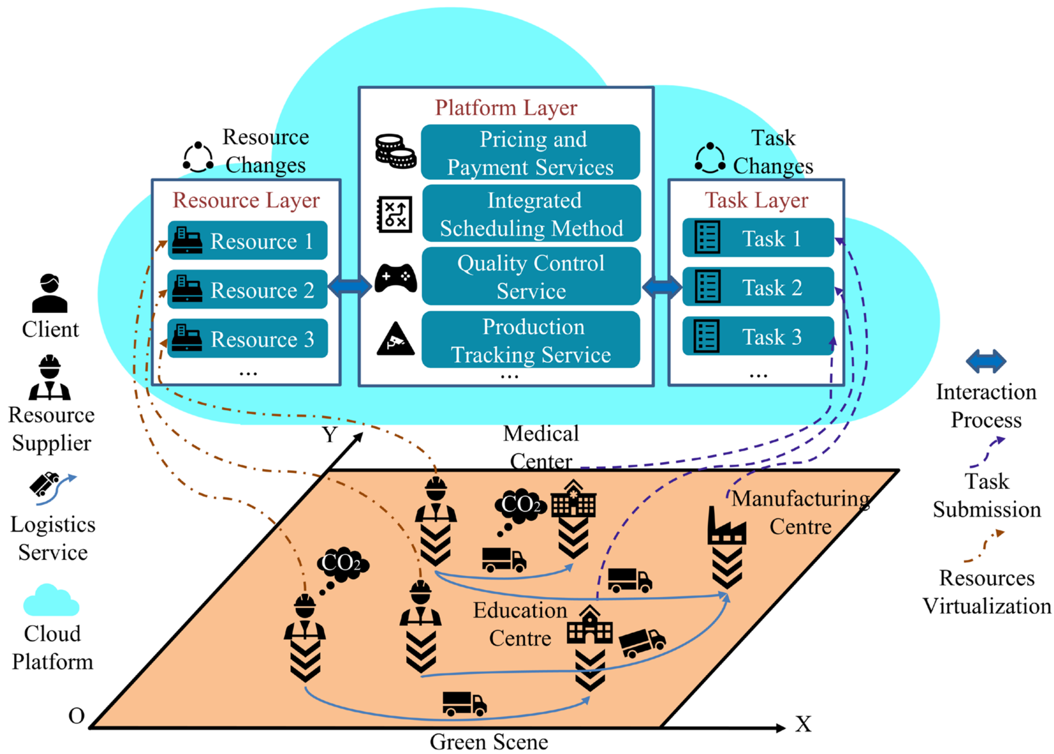

RELATED RESEARCH

This research explores 3DPCP task scheduling, specifically considering the complexities arising from multi-dynamic information perturbation in green scenes. In this section, we first decompose the 3DPCP task scheduling problem and then explore the current research progress in this area. On this basis, we analyze the difficulties encountered in 3DPCP task scheduling within green scenes. Finally, we summarize the deficiencies of the existing literature.

3DPCP Task Scheduling Problem Decomposition

3DPCP task scheduling is complex research consisting of multiple subproblems. Initially, the challenge is to intelligently match multiple products with distributed printing resources. This requires considering various factors, such as the attributes of the product devices (Chergui et al., 2018; Kucukkoc, 2019), the device time window (Wu et al., 2022), and the product delivery deadline (Darwish et al., 2021). Then, the combined batch problem arises, which entails reasonably arranging the products on the processing platform of the 3DP device to improve space utilization (Araújo et al., 2019; Che et al., 2021; De Antón et al., 2022). Scholars have successively proposed two-dimensional irregular product layout methods based on a non-fitting polygon (Zhang et al., 2020), layout methods based on computer vision (Wang et al., 2019), and improved skyline-based heuristic algorithms (Wu et al., 2022). Among these, 3DP production characteristics, such as consistent product attributes in the same batch (Oh et al., 2020), production energy consumption (Karimi et al., 2021), and production carbon emissions (Jiang et al., 2022; Zhang et al., 2017), should be considered. Finally, the complex transportation logistics from suppliers to customers are pivotal. Since an order may contain multiple products and products within an order may be produced by numerous resource providers, factors like carbon emissions (Wang et al., 2019) and coordinated transport (Wu et al., 2022; Zhang, 2021) should be considered in the logistics process.

Research Progress on 3DPCP Task Scheduling

The results of reviewing the existing literature on 3DPCP task scheduling are presented in Table 1. The factors considered include authors (Au), heterogeneous devices (Des), multi-attribute tasks (Tas), arrival/delivery time constraints (Ts), task priority (Pr), device time windows (Wi), product mix (Ma), logistics optimization (Lo), green factors (Gr), dynamic scheduling (Dy), optimization objectives (Ob), and algorithms (Al). A comparison of these factors reveals the following areas for improvement in the current research:

1. Although device time windows are crucial constraints in cloud manufacturing (Ton & Zhu, 2022), and factors such as suppliers' self-use and device maintenance should be considered in 3DPCP (Wu et al., 2022), few scholars have addressed this in their research.
2. Logistics, a key aspect of 3DPCP (Zhou et al., 2018), has only been covered by a few scholars, often with some simplifications noted (Wu et al., 2022).
3. Despite the global push for green manufacturing (Cheng et al., 2022; Ren et al., 2023), few researchers have focused on low-carbon and energy-saving measures in the 3DPCP scheduling process. Darwish et al. (2021) preset energy thresholds for devices, achieving some energy savings.
4. Dynamic information perturbation is a significant challenge in 3DPCP scheduling (Wu et al., 2022). As shown in Table 1, this issue has not been adequately addressed. For instance, Wu et al. (2022) and Li et al. (2019) considered real-time order arrival during task scheduling, and Darwish et al. (2021) designed an "allocation+scheduling" approach to achieve dynamic scheduling, enhancing response rate and device load balancing.

Heuristic scheduling rule algorithms, known for their simplicity and effectiveness, offer a method for solving scheduling problems in 3DPCP (Li et al., 2023). Compared to more complex methods such as intelligent optimization algorithms (Liu & Li, 2022; Chu et al., 2023) and game theory (Tang & Zhong, 2022), heuristic rule algorithms offer faster response times and efficient problem-solving capabilities (Wang et al., 2022), particularly in complex situations like distributed resource tasks and dynamic scheduling. Darwish et al. (2021) proposed a robust online allocation algorithm and a priority-based adaptive real-time multitask scheduling algorithm to address the optimal allocation and real-time requirements of 3DP tasks. Their simulation experiments demonstrated that this method has superior response speed and processing capability under high-load environments. Wu et al. (2022) designed a heuristic scheduling method for random task arrival scenarios and tested its performance on various instance sizes. The simulation results showed that the algorithm effectively solves the 3DPCP online scheduling problem. Li et al. (2019) proposed a policy-based heuristic decision-making method to solve the dynamic order acceptance and scheduling problem in the on-demand production of powder bed fusion systems. Experimental validation confirmed the method's favorable outcomes.

3DPCP Scheduling Difficulties in Green Scenes

Scene-driven is a new paradigm that tailors services to specific needs within a given context, promoting deep business development and industry integration (Yin et al., 2022). In this framework, the green scene further delineates sustainability and environmental concerns, aiming to promote scenario development more sustainably by using ecological materials, energy savings, emission reduction, and industrial interconnection. Current research on scheduling in green scenes focuses on energy scheduling (Hirwa et al., 2023; Kang et al., 2023), production scheduling (Li & Zhou, 2023), and logistics scheduling (Liu et al., 2023). These studies aim to create more eco-friendly, sustainable, and efficient scheduling systems that reduce energy consumption and greenhouse gas emissions. For

Table 1. Related literature

Au	Des	Tas	Ts	Pr	Wi	Ma		Gr	Dy	Ob	Al
Darwish et al. (2021)	√	√	√	√	×	√	√	Energy saving	√	/	Online allocation & ARMPS
Wu et al. (2022)	√	×	√	×	√	√	√	×	Order changes	$\mathrm{Min}(\frac{C}{V})$	Heuristic
Zhou et al. (2018)	√	√	√	√	×	√	√	×	×	$\mathrm{Min}\overline{F}$	3DPSS (Genetic algorithm)
Li et al. (2019)	√	×	√	×	×	√	×	×	Order changes	$\mathrm{Max}(APT)$	Heuristic
Liu et al. (2021)	√	√	×	×	×	×	√	×	×	$\mathrm{Min}\overline{T}$ & $\overline{C}$ $\mathrm{Max}\overline{Q}$	Genetic algorithm
Wang et al. (2019)	×	√	×	√	×	√	×	×	×	$\mathrm{Min}(PD)$	Computer vision algorithm

Note. ARMPS = adaptive real-time multitask scheduling algorithm.

instance, Darwish et al. (2021) proposed a real-time green-aware multitask scheduling architecture for personalized 3DP tasks in sustainable Industry 4.0 contexts, considering device energy consumption, high-load environments, task attributes, and real-time performance. Jin and Gao (2023) investigated the hybrid optimization problem of green supply chain networks with distributed 3D printing intelligent factory scheduling, considering carbon emissions and cost factors. However, these studies have not fully addressed the impact of the green scene on 3DPCP scheduling.

Research Review

Our systematic literature review shows that while many scholars have studied 3DPCP task scheduling, the research on 3DPCP task scheduling considering multi-dynamic information in green scenes is still insufficient. First, the impact of green scenes on 3DPCP scheduling has not been clarified, and the difficulties of 3DPCP task scheduling in green scenes remain unresolved. Second, although 3DPCP task scheduling is inherently dynamic and complex, few studies comprehensively address the multi-dynamic information involved. The integration of multiple entities and sub-problems within 3DPCP task scheduling needs further improvement and optimization. Finally, regarding research methodology, there is a lack of intelligent model algorithms to address the 3DPCP task scheduling problem considering multi-dynamic information in green scenes. Thus, there is an urgent need to explore methodologies for 3DPCP task scheduling that consider multi-dynamic information in green scenes. This exploration should be based on the correlation of 3DPCP task scheduling sub-problems, the shortcomings of current research, and the specific challenges of 3DPCP scheduling in green scenes.

PROBLEM STATEMENT

The scheduling process of 3DPCP considering multi-dynamic information perturbation in green scenes is complex and dynamic. To clearly illustrate the process, Figure 2 provides a visual representation. The specific steps are as follows:

First, the service demander ($D = \{1, 2, \ldots, d_n\}$) can send order information to the cloud platform at any time, and the number of products in the order is n_d^{pro}. The order information includes not only product information ($P = \{1, 2, \ldots, i_n\}$), such as the length, width, height, quality (l_i, w_i, h_i, q_i), printing material (Ma_i), and precision (Ac_i), but also information including the order release time (T_i^{release}) and

Figure 2. Flowchart of 3DPCP task scheduling considering multi-dynamic information perturbation in green scene

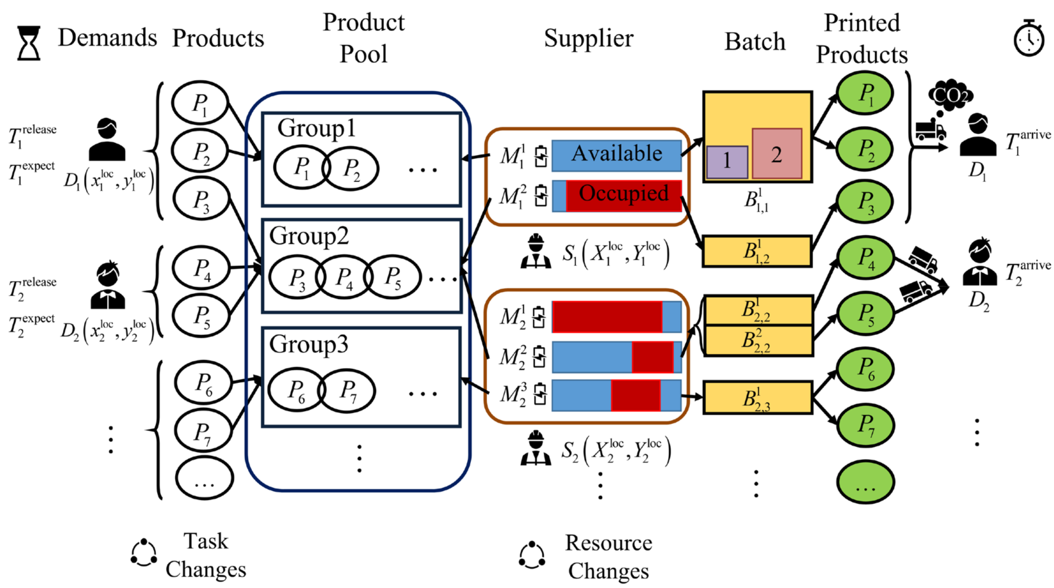

the expected delivery time (T_i^{expect}). The platform transfers all product information to the product pool (P_pool) and divides it into groups (G_{ma}^{ac}) based on the product print material and print accuracy.

Then, the scheduling mechanism is triggered when the resource supplier ($S = \{1, 2, \dots, s_n\}$) possesses devices ($M_s = \{1, 2, \cdots, m_s^n\}$) in a producible state, indicated by the nonempty set of producible devices (M_F). Each device within M_F is polled, and the products within the G_{ma}^{ac} corresponding to the device are categorized into multiple optional batches based on attributes such as the device's power of the preparation, scanning, recoating, and post-processing phases ($J_{s,m}^{\text{pre}}, J_{s,m}^{\text{scan}}, J_{s,m}^{\text{recoat}}, J_{s,m}^{\text{post}}$), carbon emissions per unit of electricity ($M_{s,m}^{\text{e/p}}$), cost of printing per unit of weight ($M_{s,m}^{\text{c/q}}$), cost of renting the device per unit of time ($M_{s,m}^{R}$), the length, width, and height of the device's processing platform ($L_{s,m}$, $W_{s,m}, H_{s,m}$), and the time window of the device ($M_{s,m}^{W} = \{1\ 2\ \cdots, M_{s,m}^{W,n_t}\}, M_{s,m}^{W,n_t} = [ws_{s,m}^{n_t}, we_{s,m}^{n_t}]$). The best batch ($b_{best}$) pairing is selected from the polling results for production. The actual production batch sequence of the device is recorded as $B_{s,m} = \{1, 2, \cdots, b_{s,m}^n\}$. The scanning and recoating time required to produce the i^{th} product are denoted as $T_i^{\text{scan}}$and T_i^{recoat}. Similarly, the scanning and recoating time needed for producing batch b on device m under supplier s are denoted as $T_{b(s,m)}^{\text{scan}}$ and $T_{b(s,m)}^{\text{recoat}}$. The pre-production preparation time and post-production processing time for the production of batch b on machine m under supplier s are denoted as $T_{b(s,m)}^{\text{pre}}$ and $T_{b(s,m)}^{\text{post}}$. The time at which batch b is finished and the time required to produce batch b on device m under supplier s are denoted as $T_{b(s,m)}^{p}$ and $T_{b(s,m)}$.

Finally, the ordered products are delivered to the service demander. The actual delivery time is denoted as T_i^{arrive}. The geographic coordinates of the supplier are (X_s^{loc}, Y_s^{loc}), the geographic coordinates of the demander are ($x_d^{\text{loc}}, y_d^{\text{loc}}$), and the time, cost, and carbon dioxide (CO_2) emissions per unit of transport distance are τ, σ, θ. Moreover, the penalty cost per unit of the delayed delivery time of the products (η_i) in the order is much higher than the logistics cost. Thus, the completed products must be dispatched earlier if the order includes products that do not meet the expected delivery time. Furthermore, not all products for service demander d are produced by the same resource supplier. Therefore, the distance and the number of transports between the supplier and the demander are denoted as $diss_{s,d}$ and $n_{s,d}^{\text{log}}$.

MATHEMATICAL MODEL

Assumptions Setting

1. To meet the product printing quality requirements, the product printing direction is pre-determined (Taufik & Jain, 2013). To save the algorithm running time, each product is arranged based on the two-dimensional minimum bounding rectangle projection in the layer direction (Wu et al., 2022).
2. Orders arrive randomly and will be returned if they contain products that do not meet the production requirements. Moreover, a 5-mm spacing is set during the product layout process to prevent damage caused by contact between products (Zhang et al., 2020).
3. A machine can only produce one batch at a time, and a batch can cover multiple products simultaneously. However, new products cannot be added during the batch production process.
4. All devices are available during the device time window. After completing a printing batch, they quickly enter the next batch production by replacing the printing tray (Wu et al., 2022).
5. Stereolithography (SLA) technology has significant advantages in large-scale production and precision manufacturing (Jung et al., 2023). Moreover, among many additive manufacturing technologies, SLA technology has the advantage of low carbon emissions and energy consumption both in standby and working conditions (Elbadawi et al., 2023). Therefore, this research is based on SLA technology.
6. The power consumed by each device at different stages of the production process is constant and unaffected by factors such as device aging and ambient temperature. Moreover, the carbon emissions and time consumed in the transport process are only related to the distance. They are not affected by factors such as traffic conditions and transport means.

Objective Function Setting

Given that cost is a vital control issue for companies (Nestorenko et al., 2022) and given the need for CO_2 reduction in green scenes (Wang & Lin, 2023), two objective functions are established:

1. **Minimize average cost per unit of product quality:** Cost is a primary concern for 3DPCP. The average cost per unit of product quality (C) is shown in Equation 1, which includes printing materials cost (C^{print}), device rental cost (C^{rent}), delay penalty cost (C^{punish}), and logistics cost (C^{log}).

$$C = (C^{\text{print}} + C^{\text{rent}} + C^{\text{punish}} + C^{\text{log}}) / \sum_{i \in P} q_i \tag{1}$$

2. **Minimize average CO_2 emissions per unit of product quality:** Low carbon emissions and energy-saving efforts are important indicators in green scenes. The average CO_2 emissions per unit of product quality (E) is shown in Equation 2, which includes CO_2 emissions in the production phase (E^{pro}) and CO_2 emissions in the logistics phase (E^{log}).

$$E = (E^{\text{pro}} + E^{\text{log}}) / \sum_{i \in P} q_i \tag{2}$$

Constraint Function Setting

Dynamic Constraints

$$P(t) = P(t-1) + \Delta P(t) \tag{3}$$

$$S(t) = S(t-1) + \Delta S(t) \tag{4}$$

$$M_s(t) = M_s(t-1) + \Delta M_s(t); \forall s \in S \tag{5}$$

$$M_{s,m}^W(t) = M_{s,m}^W(t-1) + \Delta M_{s,m}^W(t); \forall s \in S, \forall m \in M_s \tag{6}$$

Multi-dynamic information in 3DPCP within green scenes refers to the real-time changes in task and resource information during the scheduling process, which can be classified into task and resource changes. Task changes include the loaded and canceled orders (Equation 3), while resource changes include additions or deletions of suppliers (Equation 4), additions or deletions of devices supplied by suppliers (Equation 5), and device time window changes (Equation 6).

Production Constraints

$$\sum_{s\in S}\sum_{m\in M_s}\sum_{b\in B} X_{ib(s,m)} = 1; \forall i \in P \tag{7}$$

$$\sum_{i\in P} Y_{id} = n_d^{pro} \geq 1; \forall d \in D \tag{8}$$

$$\sum_{s\in S}\sum_{m\in M_s}\sum_{b\in B} Z_{b(s,m)} = 0 \tag{9}$$

Based on the SLA machining process characteristics, the following production constraints are established: Equation 7 ensures that each product can only be assigned to one batch, and each batch can only be assigned to one device from one supplier. Equation 8 guarantees that each order a service requester provides contains at least one printed product. Equation 9 ensures that the material and accuracy of the product are consistent within each batch in each device of each supplier. In the equations, $X_{ib(s,m)}$, Y_{id}, and $Z_{b(s,m)}$ are selection variables, where $X_{ib(s,m)}$ equals 1 if the i^{th} product is produced in the b^{th} batch on the m_s device, and 0 otherwise; Y_{id} equals 1 if the i^{th} product is in the d^{th} service requester order, and 0 otherwise; and $Z_{b(s,m)}$ equals 0 if the material and accuracy of the products within the b^{th} batch on the m_s device are consistent and 1 otherwise.

$$Ma_i = Ma_{s,m}; \forall i \text{ is produced on } m_s \tag{10}$$

$$Ac_i = Ac_{s,m}; \forall i \text{ is produced on } m_s \tag{11}$$

Next, the multiple types of eco-friendly materials for printing in the green scene prompt a wide range of printing task types, and different tasks have specific printing materials and accuracies. Changing device materials requires tedious steps such as emptying, cleaning, and parameter adjustment; thus, it is assumed that the print material of the 3DP device remains unchanged. The print material required for the product must match the device (Equation 10), and accuracy adjustments will have some effect on print quality. Thus, it is assumed that the print accuracy of the 3DP device is constant. The print accuracy required for the product must match the device Equation 11.

$$M_{s,m}^{\min,\mathrm{xyz}} \leq P_i^{dot,xyz} \leq M_{s,m}^{\max,\mathrm{xyz}}; \forall dot \in i; \forall i \text{ is produced on } m_s \tag{12}$$

$$i_1 \cap i_2 = \varnothing, \forall i_1, i_2 \in P, i_1 \neq i_2 \tag{13}$$

Equation 12 indicates that the coordinates of any *dot* on product *i* produced by machine m_s must be in the machine processing space. This ensures that all products must be arranged in the processing plane of the 3DP device. Equation (13) ensures that the projections of the products on the processing plane do not overlap to prevent damage caused by products contacting each other during production.

Logistics Constraints

$$n_{s,d}^{\mathrm{pro}} = \sum_{i \in P} \sum_{m \in M_s} \sum_{b \in B} X_{ib(s,m)} Y_{id} \tag{14}$$

$$\mathrm{Pun}_i = \mathrm{IF}\left(T_i^{\mathrm{arrive}} < T_i^{\mathrm{expect}}, 0, 1\right) \tag{15}$$

$$n_{s,d}^{\mathrm{pp}} = \sum_{i \in P} \sum_{m \in M_s} \sum_{b \in B} X_{ib(s,m)} Y_{id} \mathrm{Pun}_i \tag{16}$$

$$n_{s,d}^{\log} = \begin{cases} n_{s,d}^{\mathrm{pro}} & n_{s,d}^{\mathrm{pro}} = 0/1/n_{s,d}^{\mathrm{pp}} \\ 1 + n_{s,d}^{\mathrm{pp}} & \text{others} \end{cases} \tag{17}$$

$$dis\, s_{s,d} = \sqrt{(X_s - x_d)^2 + (Y_s - y_d)^2} \tag{18}$$

Print products within an order have multi-attribute characteristics; thus, the same supplier may not produce all products in an order. Therefore, the demander may have logistics relationships with multiple suppliers. Next, because delay penalties are much more expensive than transport costs, when some of the products within an order cannot be delivered on time, the completed products within the order should be dispatched in advance. The number of transports required between the demander *d* and the supplier *s* is calculated using Equation 17, where $n_{s,d}^{\mathrm{pro}}$ denotes the number of products within the order produced by supplier *s* (Equation 14) and $n_{s,d}^{\mathrm{pp}}$ denotes the number of products of demander *d* produced by resource supplier *s* that will be delivered late (Equation 16). Pun_i equals 1 if product *i* is delivered late and 0 otherwise (Equation 15). The distance between demander *d* and supplier *s* is calculated using Equation 18.

Time Constraints

$$T_{b(s,m)}^{\text{recoat}} = \max\left(X_{ib(s,m)} T_i^{\text{recoat}}\right), \forall i \in P \tag{19}$$

$$T_{b(s,m)}^{\text{scan}} = \sum_{i \in P} X_{ib(s,m)} T_i^{\text{scan}} \tag{20}$$

$$T_{b(s,m)} = T_{s,m}^{\text{pre}} + T_{b(s,m)}^{scan} + T_{b(s,m)}^{\text{recoat}} + T_{s,m}^{\text{post}} \tag{21}$$

$$T_{b(s,m)}^{\text{p}} = \begin{cases} T_{b(s,m)}^{\text{idle}} + T_{b(s,m)} & b = 1 \\ T_{(b-1)(s,m)}^{\text{p}} + T_{b(s,m)}^{\text{idle}} + T_{b(s,m)} & b > 1 \end{cases} \tag{22}$$

$$T_i^{\text{arrive}} = \sum_{s \in S} \sum_{m \in M_s} \sum_{b \in B} X_{ib(s,m)} \left(T_{b(s,m)}^{\text{p}} + \sum_{d \in D} Y_{id}\, dis\, s_{s,d}\, \tau \right) \tag{23}$$

$$r_i = \left(T_i^{\text{expect}} - T_i^{\text{release}}\right) / \left(T_i^{\text{arrive}} - T_i^{\text{release}}\right) \tag{24}$$

As a critical factor in the 3DPCP task scheduling process, time should be fully considered. Since SLA involves layer-by-layer recoating and one-by-one scanning, the recoating is performed only once, even if each layer contains multiple products. In contrast, the scanning needs to process each product within each layer. The total recoating time for batch b on machine m_s is determined based on the maximum recoating time of all products in the batch (Equation 19). The total scanning time is the sum of the scanning times of all products within the batch (Equation 20). Equation 21 estimates the total processing time of batch b on machine m_s based on the SLA process. Among them, preprocessing and postprocessing mainly include processes like material filling, device heating and cooling, de-supporting, and cleaning (Zhang et al., 2020). Equation 22 denotes the time point when the production of batch b on device m_s ends, where $T_{b(s,m)}^{\text{idle}}$ denotes the idle time before the production of batch b on device m_s. Equation 23 represents the actual delivery time of product i, which consists of the completion time point of the batch in which product i is located and the time spent on transport. Equation 24 represents the priority coefficient of product i, which is divided by 1. When the value is greater than 1, there is no penalty; when the value is less than 1, the smaller the value, the longer the delayed delivery time.

Cost Constraints

$$C^{\text{print}} = \sum_{i \in P} \sum_{s \in S} \sum_{m \in M_s} \sum_{b \in B} X_{ib(s,m)}\, q_i M_{s,m}^{c/q} \tag{25}$$

$$C^{\text{rent}} = \sum_{s \in S} \sum_{m \in M_s} \sum_{b \in B} M_{s,m}^{R}\, T_{b(s,m)} \tag{26}$$

$$C^{\text{punish}} = \sum_{i \in P} \max\left(T_i^{\text{arrive}} - T_i^{\text{expected}}, 0\right)\eta \tag{27}$$

$$C^{\log} = \sum_{s \in S}\sum_{d \in D} n_{s,d}^{\log} \, dis\, s_{s,d}\, \sigma \tag{28}$$

The total cost has four components. The printing cost is calculated from the product quality and the printing cost per unit quality of material of the production device (Equation 25). Rental costs are calculated from the rental cost per unit of time of the device and the total production time of the device (Equation 26). The delay penalty cost is calculated from the excess time and the unit delay time penalty cost (Equation 27). Logistics costs are calculated from the number of transports, the distance, and the transport cost per unit distance (Equation 28).

CO_2 Emissions Constraints

$$E_{b(s,m)} = \left(T_{b(s,m)}^{\text{pre}} J_{s,m}^{\text{pre}} + T_{b(s,m)}^{\text{recoat}} J_{s,m}^{\text{recoat}} + T_{b(s,m)}^{\text{scan}} J_{s,m}^{\text{scan}} + T_{b(s,m)}^{\text{post}} J_{s,m}^{post}\right) M_{s,m}^{\text{e/p}} \tag{29}$$

$$E^{\text{pro}} = \sum_{s \in S}\sum_{m \in M_s}\sum_{b \in B}\left(E_{b(s,m)}\right) \tag{30}$$

$$E^{\log} = \sum_{s \in S}\sum_{d \in D} n_{s,d}^{\log} \, dis\, s_{s,d}\, \theta \tag{31}$$

To visualize the CO_2 emissions of the 3DPCP task scheduling process, the scheduling process is divided into the production and logistics phases. Converting the energy required for production into CO_2 emissions during the production process is a recognized method of CO_2 emissions quantification and has been widely used in 3DP CO_2 emissions quantification research (Di & Yang, 2022; Jiang et al., 2022; Zhang et al., 2017). Numerous 3DP processes exist; thus, processes like fused deposition manufacturing (Karimi et al., 2021; Zhang et al., 2017) and laser additive manufacturing (Jiang et al., 2022; Yang et al., 2017) have different production subphases and varying power requirements for each phase. Therefore, based on the SLA process, each batch is divided into four substages: (1) preprocessing, (2) scanning, (3) recoating, and (4) postprocessing. The CO_2 emissions of each batch are calculated using Equation 29, and the total CO_2 emissions of the production stages are calculated using Equation 30. Moreover, CO_2 emissions in the logistics phase are determined by the distance and number of transports between the supplier and the client, as calculated using Equation 31.

HEURISTIC TASK SCHEDULING STRATEGY

In this section, we design a heuristic task scheduling strategy (HOS), as shown in Figure 3. This strategy consists of three nested algorithms: dynamic response, scheduling mechanism, and arrangement strategy.

Algorithm 1: Dynamic Response

The primary role of Algorithm 1 (dynamic response) is to receive and process the multi-dynamic information in the 3DPCP green scene. At the start of the cycle, the first step is to query the resource and task information base, followed by real-time responses to resource or task changes. If dynamic

Figure 3. Heuristic task scheduling strategy

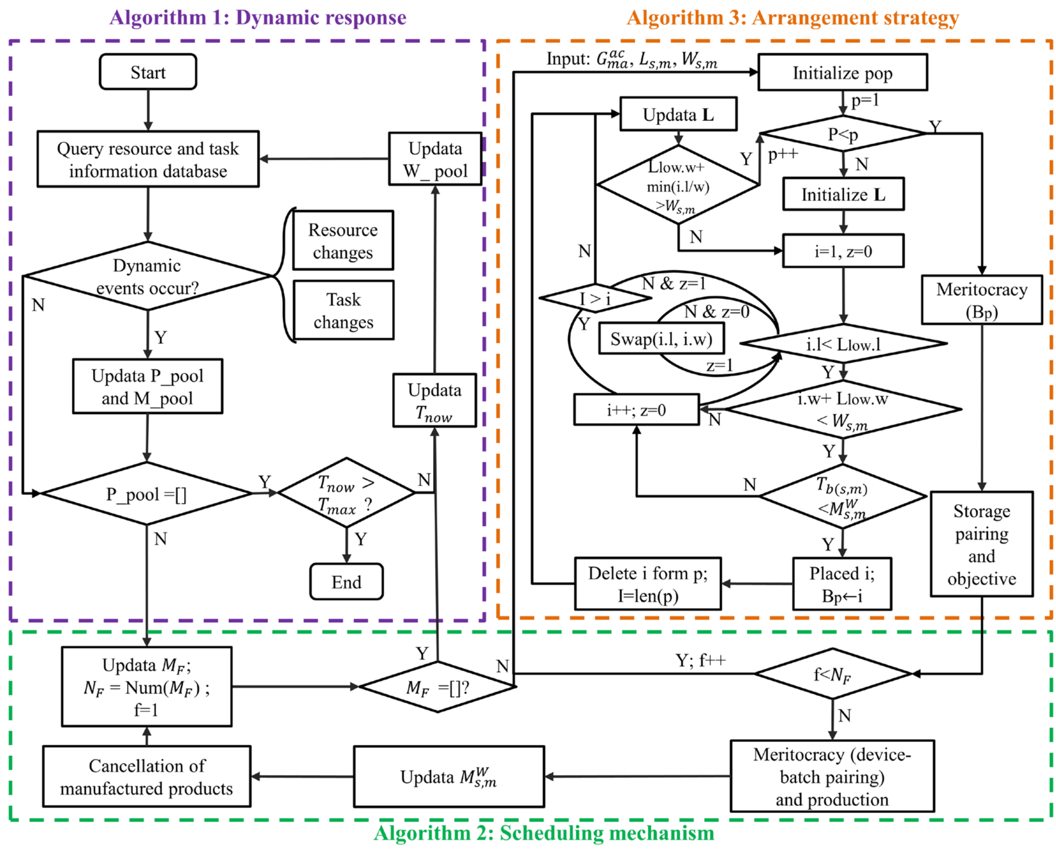

information is received, the product pool (P_pool) and resource pool (M_pool) are updated accordingly. If a breakdown occurs in the device under production, the unfinished products should be returned to the P_pool. In case of an order cancellation, whether the ordered product has entered production should be queried. If so, it cannot be cancelled; otherwise, the ordered product is removed from the P_pool. Next, it is checked whether the P_pool is empty. If not, Algorithm 2 (scheduling mechanism) is executed. If it is empty, further assessment is needed to judge whether the current moment (T_{now}) exceeds the maximum simulation time (T_{max}). If it does, the scheduling process ends; otherwise, T_{now} and the device time window pool (W_pool) are updated, and the algorithm returns to the first step of Algorithm 1.

Algorithm 2: Scheduling Mechanism

Algorithm 2 (scheduling mechanism) optimizes the matching of devices within the idle device set (M_F) to batches, where M_F denotes an idle device and corresponds to G_{ma}^{ac} nonempty. The first step is to update M_F, calculate the number of idle devices (N_F), and initialize the idle device index (f = 1). Then, it is judged whether M_F is empty. If so, the algorithm returns to Algorithm 1 (dynamic response). Otherwise, Algorithm 3 (arrangement strategy) is executed. For each index f within M_F, the corresponding $M_{s,m}$ is polled to get the optimal device–batch pair and its target value for each device within M_F. The optimal device–batch pair is selected for production through a meritocracy mechanism. Then, the time window of the corresponding device is updated according to Equation

32, and any products entering production are canceled. Finally, the algorithm returns to the first step of Algorithm 2.

$$M_{s,m}^{W,n_t} = [T_{b(s,m)}^{p}, we_{s,m}^{n_t}] \tag{32}$$

Algorithm 3: Arrangement Strategy

Algorithm 3 (arrangement strategy) addresses the product mix problem in 3DPCP task scheduling, achieving excellent optimization results. Its input parameters are G_{ma}^{ac}, $L_{s,m}$, and $W_{s,m}$. The process begins by initializing the population using a hybrid initialization population strategy that considers transport distance, delivery time, and height. The population under this strategy consists of four components:

1. **Transport distance sorting:** Products within a single individual are ordered according to the transport distance from nearest to farthest. The distance between the supplier and the demander significantly affects scheduling costs and CO_2 emissions.
2. **Delivery time sorting:** Products are prioritized based on their proximity to the delivery time, reducing penalty costs. Products within an individual are ordered according to delivery time from closest to furthest.
3. **Height sorting:** Based on Equation 19, the product with the longest recoating time in the batch determines the recoating time of the batch. Recoating time is directly proportional to the product's height, and the device's working time affects its energy consumption and rental costs. Therefore, products are sorted within an individual according to their height.
4. **Hybrid sorting:** Instead of random sorting, hybrid sorting is used. This involves individuals produced by precedence operation crossover (Zheng et al., 2014) of the individual's transport distance, delivery time, and height.

Then, the lowest horizontal line set (L) is initialized, and each individual is polled. The best batch and its target value are selected for storage through a meritocracy mechanism based on calculating the target value in the overall production environment. A modified lowest horizontal line algorithm is used to arrange the products during the individual polling process. This algorithm sequentially visits each product within an individual, making decisions based on the height and width of the lowest horizontal line, time window judgments, and a rotation mechanism. The process ends when the sum of the width of the lowest horizontal line and the smallest width/length of the non-discharged product is greater than the width of the device's processing platform. Finally, the algorithm outputs the best device–batch pairing when each individual is polled.

Meritocracy Mechanism

3DPCP task scheduling considering multi-dynamic information in the green scene is a multi-objective optimization problem, making it impossible to select the optimal solution directly from the solution set. Therefore, a meritocracy mechanism is designed to identify the dominant relationship between the solutions in the multi-objective problem by fast nondominated sorting. Subsequently, the optimal solution is selected from the set of nondominated solutions using the technique of order preference similarity to the ideal solution (TOPSIS) method. Fast nondominated sorting means that when the objective values $U_u(p_1)$ and $U_u(p_2)$ of individuals p_1 and p_2 satisfy Equation 33, then p_1 is considered to dominate p_2. If no individual dominates after polling each individual p_1, then p_1 is called the optimal individual, and the set of all optimal individuals is called the set of nondominated solutions (NS). After obtaining NS, the optimal solution is obtained using Equation 34. The technique of order preference similarity to the ideal solution TOPSIS method is a multi-attribute decision analysis method that aims to select the best solution close to the ideal solution and far from the negative ideal solution for each attribute (Behzadian et al., 2012).

$$\begin{cases} U_u(p_1) \leq U_u(p_2), & \forall u \in \{1,2\} \\ U_u(p_1) < U_u(p_2), & \exists u \in \{1,2\} \end{cases} \tag{33}$$

$$\text{opt} = \begin{cases} \text{NS} & \text{numel(NS)} = 1 \\ \text{Topsis(NS)} & \text{numel(NS)} \geq 2 \end{cases} \tag{34}$$

EXPERIMENTAL DESIGN

Given the current existence of multiple 3DP processes, obtaining directly comparable experimental results is difficult. Moreover, 3DP production is slow, and conducting various comparative experiments is time-consuming and costly. Therefore, numerical simulation experiments are employed to test the effectiveness of the proposed algorithmic model.

First, to ensure the universality and credibility of the experiment, a product information base and a machine information base are established. Product models with specific printing materials, accuracy, and size are randomly downloaded from major model websites, mainly automotive parts, industrial equipment, and artistic sculptures. From a device selection perspective, different types of SLA devices are randomly selected, which differ in processing platform size, printing cost per unit quality, rental cost, accuracy, speed, and power. Support structures are generated for each product via Materialise Magics 26.01 software, and scanning and recoating times for each product are estimated (Campbell et al., 2008). Based on this, the demander's order comprises n_d^{pro} products randomly selected from the product information base. Each order has different characteristics, such as release time, expected delivery time, dispatch location, and delay penalty cost. The supplier's device set consists of n_s^{mac} devices randomly selected from the machine information base. Each supplier has a different geographic location, CO_2 emissions per unit of electricity, device time window, and other relevant parameters.

Second, to highlight the multi-dynamic information in the 3DPCP and ensure the experiment's reliability, random ranges for simulation parameters are determined (see Table 2), and multiple sets of comparable instances are designed (see Table 3). In Table 2, the random ranges of the simulation parameters are set according to reality and references (Elbadawi et al., 2023; Jiang et al., 2022; Kellner & Igl, 2015; Wu et al., 2022), with parameters randomized within the ranges in steps. In Table 3, each instance has a different maximum simulation time ($T_{\max}$), order quantity, supplier quantity, and dynamic information perturbation quantity. Within $T_{\max}$, orders are released to the cloud platform at random time points, allowing multiple orders to be uploaded simultaneously. Supplier quantity indicates the number of suppliers at the initial moment. During $T_{\max}$, resource changes will occur at randomly selected time points, including additions or deletions of supplier devices and changes in device time windows. If the device being produced withdraws its supply, the unfinished product must be returned to the P_pool to await reallocation, with this cost being covered by the supplier. The algorithm's scheduling effect in different scenarios, such as time length, order size, resource size, and dynamic information frequency, can be effectively tested by comparing 12 sets of instances, and the experiment is repeated 15 times for each set of instances, which makes the experiment highly reliable. The test data sets and all results have been uploaded to https://pan.baidu.com/s/1__yLYn6QqY5Bgo8uI5MJGg?pwd=vx1v.

Finally, to verify the effectiveness and superiority of the proposed algorithm, we analyzed it and compared it with the state-of-the-art scheduling method in the field, Heuristic (Wu et al., 2022). However, because Heuristic does not consider machine changes, comparisons are made only

Table 2. Simulation parameters

Parameters	Random range, step	Parameters	Random range, step
$T_{\max}$ (h)	[48,432],48	$M^{R}_{s,m}$	[20,50],1
$(X_s,Y_x),(x_d,y_d)$	[1,500],1	ω(h/km)	0.06
$M^{e/p}_{s,m}(\mathrm{gCO_2/kwh})$	[200,500],1	$\theta(\mathrm{gCO_2/km})$	10
T^{expect}_{i}(h)	$[T^{\mathrm{release}}_{i}+24,\ T^{\mathrm{release}}_{i}+72]$,1	σ(/km)	0.6
n^{mac}_{s}	[1,3],1	η(/h)	[20,50],1
n^{pro}_{d}	[1,3],1	$Ma_i,Ma_{s,m}$	[1,4],1
n_t	[1,9],1	$Ac_i,Ac_{s,m}$ (mm)	[0.1,0.3],0.1

Table 3. Information for test instances

Test instances	$T_{\max}$	Range of orders	Range of supplies	Range of change
1	48	[123,178]	[20,40]	0
2	96	[151,201]	[22,43]	0
3	144	[198,253]	[25,45]	0
4	192	[241,288]	[28,45]	0
5	240	[278,341]	[29,46]	0
6	288	[328,398]	[31,48]	0
7	192	[248,298]	[25,44]	[2,18]
8	240	[281,350]	[27,45]	[3,20]
9	288	[334,400]	[32,50]	[5,21]
10	336	[381,443]	[33,52]	[8,23]
11	384	[431,481]	[36,58]	[11,24]
12	432	[478,541]	[40,67]	[12,31]

in instances 1–6. Such comparisons can effectively test the overall scheduling effectiveness of the algorithms designed in this paper. In addition, genetic algorithms have shown better optimization results than other intelligent optimization algorithms in the field of 3DP scheduling (Kapadia et al., 2022; Zhang et al., 2020). Thus, the population design in Section 5.3 is replaced with a multi-objective genetic algorithm (GAOS) to test the optimization of the transport distance–delivery time–height hybrid initialization population strategy designed in Algorithm 3 (arrangement strategy). We implemented all instances of this experiment using MATLAB R2022b and ran them on a computer with an Intel(R) Core(TM) i5-7300HQ CPU @ 2.50GHz and 12GB RAM.

In sum, the order release time, order information, device information, and dynamic information in this experiment are unpredictable and consistent with reality. Moreover, this experiment has good representativeness and reliability through the comparison of multiple instances and the comparison of algorithms.

RESULTS AND DISCUSSION

Optimization Target Comparison

The simulation results for instances 1–6 are shown in Figure 4, where each set of instance results are plotted as a three-dimensional scatterplot consisting of three axes: (1) number of trials (num); (2)

Figure 4. Simulation results of instances 1–6

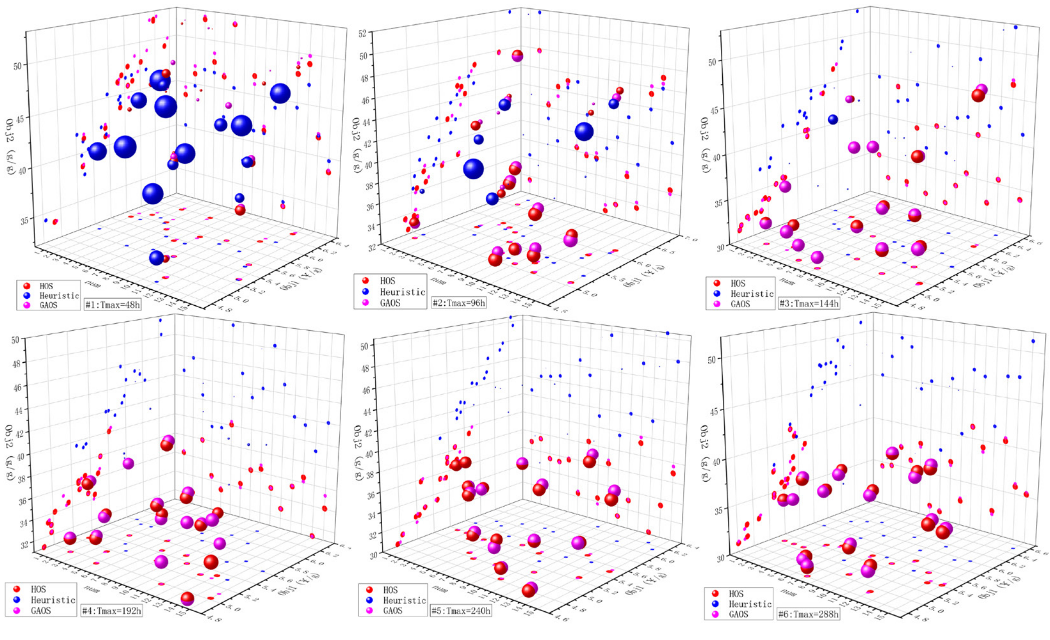

average cost per unit quality product (Obj1); and (3) average CO_2 emissions per unit quality product (Obj2). The optimization results of each algorithm are distinguished by the color of the scatter points and their projection on each plane. The scatter point size is determined according to the superiority of the optimization objective value of each strategy under each trial. Throughout instances 1–6, it can be seen that Heuristic only has better optimization results than HOS and GAOS in instance 1. With the extension of time and scale, its optimization results gradually deteriorate because Heuristic is the selection of the optimal device by the product. This can lead to the concentration of the product on the optimal device while wasting the production resources of the sub-optimal device, thus aggravating the low-supply situation when large-scale production occurs. HOS and GAOS are a combination of products that are selected by idle devices to produce the optimal device-batch pairing sequentially. The idea can prioritize the use of optimal production resources and make full use of suboptimal resources in large-scale production. Moreover, the embedded arrangement strategy in HOS and the random sorting in GAOS have a larger optimization space than the ascending order based on delivery time in Heuristic and show better optimization results in large-scale production.

The simulation results for instances 7–12 are shown in Figure 5. As the complexity of the problem increases with the continuous expansion of supplier size, order numbers, and multi-dynamic information, Heuristic can no longer adapt to the complex NP-hard problem under device fluctuations. Moreover, from the optimization results of HOS and GAOS, it can be seen that the optimization results of HOS and GAOS are similar regardless of the dynamic information perturbation. This is because the algorithmic principles of HOS and GAOS are basically the same, and GAOS simply replaces the population design in HOS with a multi-objective genetic algorithm. This shows that Algorithm 3 (arrangement strategy) has an excellent optimization effect. Among them, the initialization population strategy designed based on the 3DPCP task scheduling characteristics considering multi-dynamic information in green scenes can generate excellent populations. This can replace the population migration and iteration process of intelligent optimization algorithms to reduce the algorithm complexity. In addition, by analyzing instances 4–9 and 7–12, it can be seen that in the case with the same simulation time but with or without resource changes, and in the case with resource changes

Figure 5. Simulation results of instances 7–12

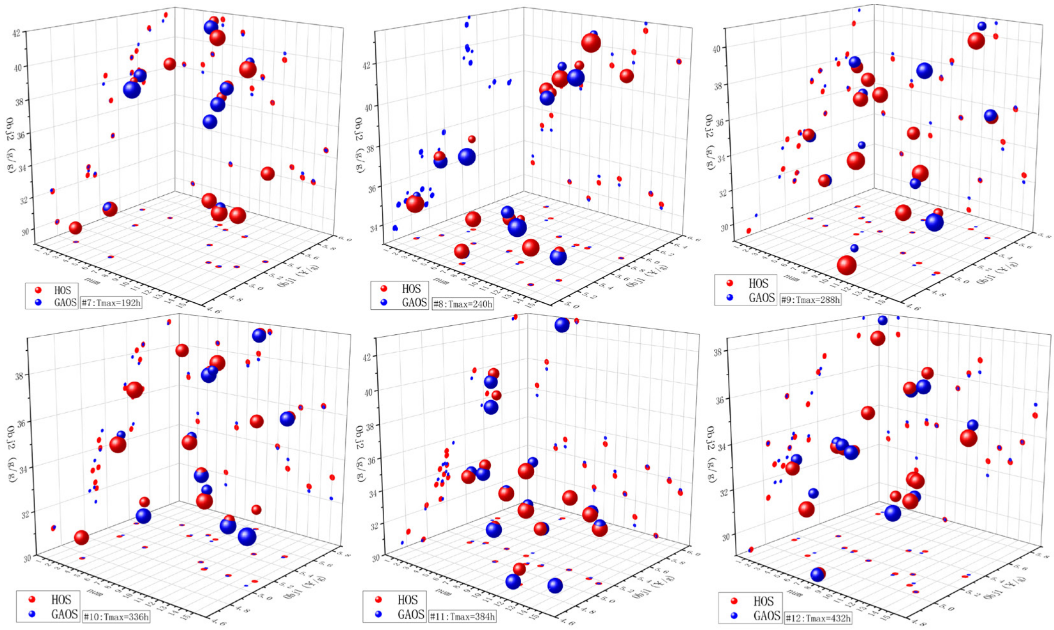

but with the gradual expansion of the experimental scale, the optimization results obtained by HOS is stable, which shows that the algorithms have a strong ability to deal with resource changes and large-scale production.

Key Indicators Comparison

A fast solving speed can instantly respond to dynamic information and make real-time decisions, and a shorter product delivery cycle can improve customer satisfaction. Therefore, solving speed and product delivery cycle are important indicators in this experiment. The average solving time ((1) $\overline{T}_{run}(s)$) and average product delivery cycle ((2) $\overline{T}_{cycle}(h)$) for different algorithms under each instance are shown in Table 4.

$\overline{T}_{run}(s)$ is the average solving time of the 15 trials of the algorithm in the instances. As shown in Table 4, HOS had the fastest solution speed, Heuristic was the second fastest, and GAOS was the slowest. This is because HOS polls for idle devices and selects the optimal device–batch pair to produce when there are idle devices. Additionally, the initialized population strategy in HOS replaces the population's migration and iteration, saving solving time and improving the optimization capability. Moreover, the solving time allocation to each scheduling trigger in HOS will be smaller, which is acceptable in real production scenarios. Heuristic is a process that polls each unproduced product, puts it into the selectable devices, calculates the objective value, and then places the product in the optimal device by comparing the objective values. In this process, the objective value calculation is performed for each placement. On the other hand, GAOS consumes much time in the process of population iteration and target value calculation. $\overline{T}_{cycle}(h)$ is the average of the product delivery cycles for the 15 algorithm trials in the instances. As shown in Table 4, HOS and GAOS had shorter average product delivery cycles, while Heuristic had the longest. This is because the scheduling rules of HOS and GAOS make the best use of resources, allowing products to be produced and delivered quickly. Heuristic can result in concentrating the production of products on the optimal device, thereby wasting suboptimal resources and leading to longer product delivery times.

Table 4. (1) $\overline{T_{run}}$ and (2) $\overline{T_{cycle}}$ for Each algorithm

Indicators	(1)	(2)	(1)	(2)	(1)	(2)	(1)	(2)
T_{max} Algorithm	48		96		144		192	
HOS	10.55	16.89	14.13	14.64	24.63	12.89	32.65	12.68
Heuristic	46.34	20.73	40.21	19.00	64.77	18.31	78.40	18.56
GAOS	93.19	17.02	121.39	14.67	203.28	12.89	265.12	12.68
T_{max} Algorithm	240		288		192		240	
HOS	35.56	12.64	57.36	12.71	30.00	12.94	42.84	13.38
Heuristic	98.73	18.78	166.85	19.16	/	/	/	/
GAOS	390.69	12.66	563.61	12.73	230.87	12.95	347.17	13.39
T_{max} Algorithm	288		336		384		432	
HOS	55.93	12.73	82.23	12.31	89.48	12.48	144.8	11.98
GAOS	493.56	12.78	746.26	12.30	815.11	12.47	1350.75	12.02

CONCLUSIONS AND PROSPECTS

This article defined a 3DPCP task scheduling problem considering multi-dynamic information in green scenes. It constructed and designed the task scheduling model and strategy, respectively, and demonstrated the effectiveness and superiority of the proposed model and strategy through simulation experiments. The main contributions of this article are as follows:

1. It defined a 3DPCP task scheduling problem considering multi-dynamic information in green scenes. This problem considers dynamic information such as order arrivals and cancellations, supplier device entries and cancellations, and device time window changes during the scheduling process. In addition, it considers the diversity of eco-friendly materials, the variability of clean energy in different regions, the synergy of production logistics, and the carbon footprints of each link in the green scene.
2. It developed a task scheduling model to minimize the average cost and CO_2 emissions per unit quality product. This model considers dynamic constraints associated with real-time changes in tasks and resources, as well as two-dimensional rectangular constraints in product mix batches, logistics constraints, and time, cost, and carbon emission constraints.
3. It designed the HOS strategy. Comparative experiments demonstrated that the strategy could effectively solve the 3DPCP task scheduling problem considering multi-dynamic information perturbation in green scenes. The HOS demonstrated strong cost and CO_2 emission optimization capabilities, a faster solution speed, and a shorter product delivery cycle.

Although this method can effectively solve this problem, future research should explore business model innovations brought by the industry interconnection to 3DPCP within green scenes. Moreover, the proposed model algorithm can be expanded from multiple perspectives as the model evolves. In the production stage, problems like the 3D combination method of irregular products, the optimization of product layering direction, and the support structure design are integrated into the model and algorithms. This helps to improve the space utilization rate. In the logistics stage, merging overlapping routes can save logistics transport distance.

AUTHOR NOTE

Jianjia He *https://orcid.org/0000-0001-5987-3605*; Jian Wu *https://orcid.org/0000-0001-9783-0251*; Keng Leng Siau https://orcid.org/0000-0001-8139-4467.

Jianjia He and Jian Wu are now at the Business School, University of Shanghai for Science and Technology. Keng Leng Siau is now at the City University of Hong Kong's Department of Information Systems.

The authors of the publication declare there are no competing interests. The work was supported by the National Natural Science Foundation of China [grant number 71871144], Shanghai Philosophy and Social Science Planning [grant number 2023BGL009], and the Science and Technology Development Project of the University of Shanghai for Science and Technology [grant number 2020KJFZ046].

Data are available upon request from the authors. Correspondence concerning this article should be addressed to Keng Leng Siau at klsiau@cityu.edu.hk.

PROCESS DATES

Received: April 14, 2024, Revision: May 17, 2024, Accepted: June 13, 2024

REFERENCES

Alvarez-Meaza, I., Zarrabeitia-Bilbao, E., Rio-Belver, R. M., & Garechana-Anacabe, G. (2021). Green scheduling to achieve green manufacturing: Pursuing a research agenda by mapping science. *Technology in Society*, *67*, 101758. 10.1016/j.techsoc.2021.101758

Araújo, L. J. P., Özcan, E., Atkin, J. A. D., & Baumers, M. (2019). Analysis of irregular three-dimensional packing problems in additive manufacturing: A new taxonomy and dataset. *International Journal of Production Research*, *57*(18), 5920–5934. 10.1080/00207543.2018.1534016

Behzadian, M., Otaghsara, S. K., Yazdani, M., & Ignatius, J. (2012). A state-of-the-art survey of TOPSIS applications. *Expert Systems with Applications*, *39*(17), 13051–13069. 10.1016/j.eswa.2012.05.056

Campbell, I., Combrinck, J., de Beer, D., & Barnard, L. (2008). Stereolithography build time estimation based on volumetric calculations. *Rapid Prototyping Journal*, *14*(5), 271–279. 10.1108/13552540810907938

Che, Y., Hu, K., Zhang, Z., & Lim, A. (2021). Machine scheduling with orientation selection and two-dimensional packing for additive manufacturing. *Computers & Operations Research*, *130*, 105245. 10.1016/j.cor.2021.105245

Cheng, Z., Wang, L., & Zhang, Y. (2022). Does smart city policy promote urban green and low-carbon development? *Journal of Cleaner Production*, *379*, 134780. 10.1016/j.jclepro.2022.134780

Chergui, A., Hadj-Hamou, K., & Vignat, F. (2018). Production scheduling and nesting in additive manufacturing. *Computers & Industrial Engineering*, *126*, 292–301. 10.1016/j.cie.2018.09.048

Chu, J., Tan, S., Lin, J., Chan, J. H. T., Lee, L. Y. S., & Zheng, L. J. (2023). Optimizing fresh agricultural product distribution paths under demand uncertainty: A particle swarm optimization-based algorithm. [JGIM]. *Journal of Global Information Management*, *31*(1), 1–22. 10.4018/JGIM.326557

Cui, J., Ren, L., Mai, J., Zheng, P., & Zhang, L. (2022). 3D printing in the context of cloud manufacturing. *Robotics and Computer-integrated Manufacturing*, *74*, 102256. 10.1016/j.rcim.2021.102256

Darwish, L. R., El-Wakad, M. T., & Farag, M. M. (2021). Towards sustainable industry 4.0: A green real-time IIoT multitask scheduling architecture for distributed 3D printing services. *Journal of Manufacturing Systems*, *61*, 196–209. 10.1016/j.jmsy.2021.09.004

De Antón, J., Villafáñez, F., Poza, D., & López-Paredes, A. (2022). A framework for production planning in additive manufacturing. *International Journal of Production Research*, *61*(24), 1–18.

Di, L., & Yang, Y. (2022). Greenhouse gas emission analysis of integrated production-inventory-transportation supply chain enabled by additive manufacturing. *Journal of Manufacturing Science and Engineering*, *144*(3), 031006. 10.1115/1.4051887

Elbadawi, M., Basit, A. W., & Gaisford, S. (2023). Energy consumption and carbon footprint of 3D printing in pharmaceutical manufacture. *International Journal of Pharmaceutics*, *639*, 122926. 10.1016/j.ijpharm.2023.12292637030639

Feng, Y., Lai, K., & Zhu, Q. (2022). Green supply chain innovation: Emergence, adoption, and challenges. *International Journal of Production Economics*, *248*, 108497. 10.1016/j.ijpe.2022.108497

Hirwa, J., Zolan, A., Becker, W., Flamand, T., & Newman, A. (2023). Optimizing design and dispatch of a resilient renewable energy microgrid for a South African hospital. *Applied Energy*, *348*, 121438. 10.1016/j.apenergy.2023.121438

Jiang, X., Liu, A., Yang, G., Liu, W., Bian, H., & Suo, Y. (2022). Low-carbon modeling and process parameter optimization in laser additive manufacturing process. [in Chinese]. *Jixie Gongcheng Xuebao*, *58*(5), 223–238. 10.3901/JME.2022.05.223

Jin, Y., & Gao, C. (2023). Hybrid optimization of green supply chain network and scheduling in distributed 3D printing intelligent factory. *Sustainability (Basel)*, *15*(7), 5948. 10.3390/su15075948

Jung, S., Kara, L. B., Nie, Z., Simpson, T. W., & Whitefoot, K. S. (2023). Is additive manufacturing an environmentally and economically preferred alternative for mass production? *Environmental Science & Technology*, *57*(16), 6373–6386. 10.1021/acs.est.2c0492737066969

Kang, H., Jung, S., Kim, H., Hong, J., Jeoung, J., & Hong, T. (2023). Multi-objective sizing and real-time scheduling of battery energy storage in energy-sharing community based on reinforcement learning. *Renewable & Sustainable Energy Reviews*, *185*, 113655. 10.1016/j.rser.2023.113655

Kapadia, M. S., Uzsoy, R., Starly, B., & Warsing, D. P.Jr. (2022). A genetic algorithm for order acceptance and scheduling in additive manufacturing. *International Journal of Production Research*, *60*(21), 6373–6390. 10.1080/00207543.2021.1991023

Karimi, S., Kwon, S., & Ning, F. (2021). Energy-aware production scheduling for additive manufacturing. *Journal of Cleaner Production*, *278*, 123183. 10.1016/j.jclepro.2020.123183

Kellner, F., & Igl, J. (2015). Greenhouse gas reduction in transport: Analyzing the carbon dioxide performance of different freight forwarder networks. *Journal of Cleaner Production*, *99*, 177–191. 10.1016/j.jclepro.2015.03.026

Kucukkoc, I. (2019). MILP models to minimise makespan in additive manufacturing machine scheduling problems. *Computers & Operations Research*, *105*, 58–67. 10.1016/j.cor.2019.01.006

Li, Q., Zhang, D., Wang, S., & Kucukkoc, I. (2019). A dynamic order acceptance and scheduling approach for additive manufacturing on-demand production. *International Journal of Advanced Manufacturing Technology*, *105*(9), 3711–3729. 10.1007/s00170-019-03796-x

Li, X., Huang, J., Li, J., Li, Y. X., & Gao, L. (2023). Research and development trend of intelligent shop dynamic scheduling. [in Chinese]. *Scientia Sinica (Technologica)*, *53*(7), 1016–1030. 10.1360/SST-2022-0481

Li, Z., & Zhou, S. (2023). High dimensional multi-objective dynamic job shop scheduling optimization for green intelligent manufacturing. [in Chinese]. *Operations Research and Management Science*, *32*(1), 47–53.

Lin, B., & Ma, R. (2022). How does internet development affect green technology innovation in China? [JGIM]. *Journal of Global Information Management*, *30*(1), 1–21. 10.4018/JGIM.309081

Liu, Q., & Li, J. (2022). The progress of business analytics and knowledge management for enterprise performance using artificial intelligence and man-machine coordination. [JGIM]. *Journal of Global Information Management*, *30*(11), 1–21. 10.4018/JGIM.302642

Liu, Q., Wang, C., Li, X., & Gao, L. (2023). A multi-population co-evolutionary algorithm for green integrated process planning and scheduling considering logistics system. *Engineering Applications of Artificial Intelligence*, *126*, 107030. 10.1016/j.engappai.2023.107030

Liu, S., Zhang, L., Zhang, W., & Shen, W. (2021). Game theory based multi-task scheduling of decentralized 3D printing services in cloud manufacturing. *Neurocomputing*, *446*, 74–85. 10.1016/j.neucom.2021.03.029

Liu, Y., Wang, L., Wang, X. V., Xu, X., & Zhang, L. (2019). Scheduling in cloud manufacturing: State-of-the-art and research challenges. *International Journal of Production Research*, *57*(15–16), 4854–4879. 10.1080/00207543.2018.1449978

Nestorenko, T., Nestorenko, O., Morkunas, M., Volkov, A., Balezentis, T., Streimikiene, D., & Cai, J. (2022). Optimization of production decisions under resource constraints and community priorities. [JGIM]. *Journal of Global Information Management*, *30*(12), 1–24. 10.4018/JGIM.304066

Oh, Y., Witherell, P., Lu, Y., & Sprock, T. (2020). Nesting and scheduling problems for additive manufacturing: A taxonomy and review. *Additive Manufacturing*, *36*, 101492. 10.1016/j.addma.2020.101492

Ren, X., Qin, X., Li, Y., & Tian, Y. (2023). Impact of the digital economy on the green transformation of China's manufacturing industry: A dual perspective of technological innovation and industrial structure optimization. [JGIM]. *Journal of Global Information Management*, *31*(6), 1–22. 10.4018/JGIM.321179

Sgarbossa, F., Peron, M., Lolli, F., & Balugani, E. (2021). Conventional or additive manufacturing for spare parts management: An extensive comparison for Poisson demand. *International Journal of Production Economics*, *233*, 107993. 10.1016/j.ijpe.2020.107993

Srinivasan, R., Giannikas, V., McFarlane, D., & Thorne, A. (2018). Customising with 3D printing: The role of intelligent control. *Computers in Industry*, *103*, 38–46. 10.1016/j.compind.2018.09.003

Tan, Z., & Lin, B. (2023). Impact of carbon capture (storage) and carbon tax on economic dispatch of an integrated energy system. [JGIM]. *Journal of Global Information Management*, *31*(1), 1–21. 10.4018/JGIM.331695

Tang, X., & Zhong, T. (2022). Research on COVID-19 prevention and control model based on evolutionary games. [JGIM]. *Journal of Global Information Management*, *30*(10), 1–17. 10.4018/JGIM.300818

Taufik, M., & Jain, P. K. (2013). Role of build orientation in layered manufacturing: A review. *International Journal of Manufacturing Technology and Management*, *27*(1–3), 47–73. 10.1504/IJMTM.2013.058637

Tong, H., & Zhu, J. (2022). A novel method for customer-oriented scheduling with available manufacturing time windows in cloud manufacturing. *Robotics and Computer-integrated Manufacturing*, *75*, 102303. 10.1016/j.rcim.2021.102303

Wang, C., & Lin, B. (2023). Managing carbon efficiency and carbon equity: What information do we have from embodied carbon emissions? [JGIM]. *Journal of Global Information Management*, *31*(1), 1–22. 10.4018/JGIM.334360

Wang, J., Yao, S., Sheng, J., & Yang, H. (2019). Minimizing total carbon emissions in an integrated machine scheduling and vehicle routing problem. *Journal of Cleaner Production*, *229*, 1004–1017. 10.1016/j.jclepro.2019.04.344

Wang, X., Zhang, L., Liu, Y., Li, F., Chen, Z., Zhao, C., & Bai, T. (2022). Dynamic scheduling of tasks in cloud manufacturing with multi-agent reinforcement learning. *Journal of Manufacturing Systems*, *65*, 130–145. 10.1016/j.jmsy.2022.08.004

Wang, Y., Zheng, P., Xu, X., Yang, H., & Zou, J. (2019). Production planning for cloud-based additive manufacturing—A computer vision-based approach. *Robotics and Computer-integrated Manufacturing*, *58*, 145–157. 10.1016/j.rcim.2019.03.003

Wu, Q., Xie, N., & Zheng, S. (2022). Integrated cross-supplier order and logistic scheduling in cloud manufacturing. *International Journal of Production Research*, *60*(5), 1633–1649. 10.1080/00207543.2020.1867921

Wu, Q., Xie, N., Zheng, S., & Bernard, A. (2022). Online order scheduling of multi 3D printing tasks based on the additive manufacturing cloud platform. *Journal of Manufacturing Systems*, *63*, 23–34. 10.1016/j.jmsy.2022.02.007

Yang, Y., Li, L., Pan, Y., & Sun, Z. (2017). Energy consumption modeling of stereolithography-based additive manufacturing toward environmental sustainability. *Journal of Industrial Ecology*, *21*(S1), S168–S178. 10.1111/jiec.12589

Yin, X., Su, Y., Chen, J., & Chen, T. (2022). Context-driven innovation: Connotation, theoretical logic and practical approach. [in Chinese]. *Science & Technology Progress and Policy*, *39*(15), 1–10.

Zhang, J., Yao, X., & Li, Y. (2020). Improved evolutionary algorithm for parallel batch processing machine scheduling in additive manufacturing. *International Journal of Production Research*, *58*(8), 2263–2282. 10.1080/00207543.2019.1617447

Zhang, L., Zhang, B., Bao, H., Zhang, C., & Zhang, W. (2017). Carbon emissions quantitative methodology of product fused deposition manufacturing. [in Chinese]. *Jixie Gongcheng Xuebao*, *53*(5), 50–59. 10.3901/JME.2017.05.050

Zhang, X. (2021). B2C e-commerce logistics network optimization model. [JGIM]. *Journal of Global Information Management*, *30*(3), 1–19. 10.4018/JGIM.20220701.oa7

Zhang, Y., Du, H., Piao, T., Shi, H., & Tsai, S. B. (2024). How manufacturing companies can improve their competitiveness: Research on service transformation and product innovation based on computer vision. [JGIM]. *Journal of Global Information Management*, *32*(1), 1–26. 10.4018/JGIM.336485

Zheng, X. L., Wang, L., & Wang, S. Y. (2014). A novel fruit fly optimization algorithm for the semiconductor final testing scheduling problem. *Knowledge-Based Systems*, *57*, 95–103. 10.1016/j.knosys.2013.12.011

Zhong, R. Y., Kang, K., Yu, C., Zhang, Y., Tao, F., & Bernard, A. (2022). A resource sharing approach for PSS-enabled additive manufacturing platform. *CIRP Journal of Manufacturing Science and Technology*, *39*, 414–426. 10.1016/j.cirpj.2022.10.004

Zhou, L., Zhang, L., Laili, Y., Zhao, C., & Xiao, Y. (2018). Multi-task scheduling of distributed 3D printing services in cloud manufacturing. *International Journal of Advanced Manufacturing Technology*, *96*(9), 3003–3017. 10.1007/s00170-017-1543-z

Jianjia received a Ph.D. in management science and engineering from the University of Shanghai for Science and Technology, Shanghai, China, in 2012. He is a vice president, professor, and doctoral tutor with the Business School, University of Shanghai for Science and Technology. He is a member of the China Society of Systems Engineering and the Deputy Secretary General of the Education Systems Engineering Committee of the China Society of Systems Engineering. He has published articles in several well-known journals, such as Technological Forecasting and Social Change, Transportation Science, Energy, and others. His research interests include enterprise supply and demand networks, industrial interconnection, smart logistics and supply chain management, and intelligent manufacturing.

Jian Wu is a graduate student at the Business School of the University of Shanghai for Science and Technology, Shanghai, China. His research directions include intelligent manufacturing, intelligent scheduling, industrial interconnection, cloud platforms, and 3D printing. E-mail: 212421070@st.usst.edu.cn.

Professor Siau is the head of the Department of Information Systems and chair of information systems at the City University of Hong Kong (June 2021–present). He is editor-in-chief of the Journal of Database Management (SCI and ABDC's A journal). He is also a senior editor for the Industrial Management & Data Systems journal. Moreover, Professor Siau has more than 300 academic publications. His research publications have appeared in journals such as MIS Quarterly, Journal of the Association for Information Systems, Journal of Strategic Information Systems, Decision Support Systems, Information Systems Journal, Data and Knowledge Engineering, IEEE Transactions on Information Systems in Biomedicine, IEEE Transactions on Systems, Man, and Cybernetics, IEEE Transactions on Professional Communication, IEEE Transactions on Education, Communications of the ACM, and Communications of the AIS. According to Google Scholar, he has a citation count of more than 22,000, and his h-index and i10-index are 75 and 192, respectively.